

Scanning tunneling microscopy study on symmetry breaking of charge density wave in FeGe

Jiakang Zhang(张嘉康), Ziyuan Chen(陈子元), Xueliang Wu(吴学良), Mingzhe Li(李明哲), Yuanji Li(李元骥), Ruotong Yin(尹若彤), Jiashuo Gong(巩佳硕), Shiyuan Wang(王适源), Aifeng Wang(王爱峰), Dong-Lai Feng(封东来), and Ya-Jun Yan(闫亚军)

Citation: Chin. Phys. B, 2025, 34 (**4**): 047303. DOI: 10.1088/1674-1056/adb389
Journal homepage: http://cpb.iphy.ac.cn; http://iopscience.iop.org/cpb

What follows is a list of articles you may be interested in

Chiral phonons of honeycomb-type bilayer Wigner crystals

Dingrui Yang(杨丁睿), Lingyi Li(李令仪), Na Zhang(张娜), and Hongyi Yu(俞弘毅)
Chin. Phys. B, 2025, 34 (**1**): 017301. DOI: 10.1088/1674-1056/ad8eca

Recent progress on valley polarization and valley-polarized topological states in two-dimensional materials

Fei Wang(王斐), Yaling Zhang(张亚玲), Wenjia Yang(杨文佳), Huisheng Zhang(张会生), and Xiaohong Xu(许小红)
Chin. Phys. B, 2024, 33 (**1**): 017306. DOI: 10.1088/1674-1056/ad0713

Spin transport properties for B-doped zigzag silicene nanoribbons with different edge hydrogenations

Jing-Fen Zhao(赵敬芬), Hui Wang(王辉), Zai-Fa Yang(杨在发), Hui Gao(高慧), Hong-Xia Bu(步红霞), and Xiao-Juan Yuan(袁晓娟)
Chin. Phys. B, 2022, 31 (**1**): 017302. DOI: 10.1088/1674-1056/ac0795

Quantization of the band at the surface of charge density wave material 2H-$TaSe_2$

Man Li(李满), Nan Xu(徐楠), Jianfeng Zhang(张建丰), Rui Lou(娄睿), Ming Shi(史明), Lijun Li(黎丽君), Hechang Lei(雷和畅), Cedomir Petrovic, Zhonghao Liu(刘中灏), Kai Liu(刘凯), Yaobo Huang(黄耀波), and Shancai Wang(王善才)
Chin. Phys. B, 2021, 30 (**4**): 047305. DOI: 10.1088/1674-1056/abe9a8

Scanning tunneling microscopic investigation on morphology of magnetic Weyl semimetal $YbMnBi_2$

Zhen Zhu(朱朕), Dong Yan(严冬), Xiao-Ang Nie(聂晓昂), Hao-Ke Xu(徐豪科), Xu Yang(杨旭), Dan-Dan Guan(管丹丹), Shiyong Wang(王世勇), Yao-Yi Li(李耀义), Canhua Liu(刘灿华), Jun-Wei Liu(刘军伟), Hui-Xia Luo(罗惠霞), Hao Zheng(郑浩), Jin-Feng Jia(贾金锋)
Chin. Phys. B, 2019, 28 (**7**): 077302. DOI: 10.1088/1674-1056/28/7/077302

SPECIAL TOPIC — Recent progress on kagome metals and superconductors

Scanning tunneling microscopy study on symmetry breaking of charge density wave in FeGe

Jiakang Zhang(张嘉康)[1,†], Ziyuan Chen(陈子元)[1,†], Xueliang Wu(吴学良)[2], Mingzhe Li(李明哲)[1], Yuanji Li(李元骥)[1], Ruotong Yin(尹若彤)[1], Jiashuo Gong(巩佳硕)[1], Shiyuan Wang(王适源)[1], Aifeng Wang(王爱峰)[2], Dong-Lai Feng(封东来)[1,3,4], and Ya-Jun Yan(闫亚军)[1,4,‡]

[1] *School of Emerging Technology and Department of Physics, University of Science and Technology of China, Hefei* 230026, *China*

[2] *Low temperature Physics Laboratory, College of Physics and Center of Quantum Materials and Devices, Chongqing University, Chongqing* 401331, *China*

[3] *National Synchrotron Radiation Laboratory and School of Nuclear Science and Technology, New Cornerstone Science Laboratory, University of Science and Technology of China, Hefei* 230026, *China*

[4] *Hefei National Laboratory, University of Science and Technology of China, Hefei* 230026, *China*

(Received 14 October 2024; revised manuscript received 16 January 2025; accepted manuscript online 7 February 2025)

The complex symmetry breaking states in AV_3Sb_5 family have attracted extreme research attention, but controversy still exists, especially in the question of time reversal symmetry breaking of the charge density wave (CDW). Most recently, a chiral CDW has been suggested in kagome magnet FeGe, but the related study is very rare. Here, we use a scanning tunneling microscope to study the symmetry breaking behavior of both the short- and long-range CDWs in FeGe. Different from previous studies, our study reveals an isotropic long-range CDW without obvious symmetry breaking, while local rotational symmetry breaking appears in the short-range CDW, which may be related to the existence of strong structural disorders. Moreover, the charge distribution of the short-range CDW is inert to the applied external magnetic fields and the detailed spin arrangements of FeGe, inconsistent with the expectation of a chiral CDW associated with chiral flux. Our results rule out the existence of spontaneous chiral and rotational symmetry breaking in the CDW state of FeGe, putting strong constraints on the further understanding of CDW mechanism.

Keywords: symmetry breaking, kagome magnet, charge density wave

PACS: 73.22.Gk, 87.64.Dz, 71.45.Lr, 75.50.Ee

DOI: 10.1088/1674-1056/adb389 **CSTR:** 32038.14.CPB.adb389

1. Introduction

Electronic states in condensed matter systems generally follow certain symmetries of the underlying crystal lattice, however, spontaneous symmetry breaking occurs frequently due to the existence of appreciable many-body interactions, leading to rich emergent quantum states. For instance, ferromagnetism breaks time reversal symmetry,[1–4] superconductivity breaks U(1) symmetry,[5–9] charge density wave (CDW) breaks translational symmetry,[10–15] etc. However, in real materials, the observed symmetry breaking states are not necessarily spontaneous, and might be induced by unavoidable defects, disorders, or local strain. For example, the existence of oxygen vacancies in metal oxides often induces magnetism,[16,17] local strain can induce exotic CDW or PDW states in transition metal dichalcogenides and iron-based superconductors.[18,19] These symmetry-breaking states are completely different in origin from the spontaneous ones, thus distinguishing them is very important for revealing the more essential physical mechanism.

Kagome superconductors AV_3Sb_5 (A = Cs, K, Rb) have recently attracted extreme research attention due to the coexistence of superconductivity, CDW, nematic order and PDW all in a single material.[20–26] More specifically, the triple-Q $2\times2\times2$ CDW has been suggested to possess both the rotational symmetry breaking (RSB) and time-reversal symmetry breaking (TRSB).[22,23,27–33] The RSB in the CDW has been widely confirmed, which might be induced by a shift of complex structural distortions between adjacent kagome layers,[34–40] anisotropic electron–phonon coupling[41] and so on. As for the TRSB in the CDW, it is theoretically suggested to be related to the existence of a chiral flux phase or charge bond order with orbital currents induced by the unique sublattice structures of kagome lattice.[42–44] The chirality of orbital currents will reverse under the external/internal magnetic fields with opposite directions, leading to a chirality reversal of the associated CDW.[45–48] One manifestation of the CDW chirality is the inequivalence of CDW intensities among three propagating directions, by applying strain, polarized light, magnetic field and so on, possibly due to the unusual electrostriction or piezo-magnetic responses of the CDW and the cor-

†These authors contributed equally to this work.

‡Corresponding author. E-mail: yanyj87@ustc.edu.cn

© 2025 Chinese Physical Society and IOP Publishing Ltd. All rights, including for text and data mining, AI training, and similar technologies, are reserved.

responding lattice distortions[49,50] This allows one to define the clockwise and counterclockwise chiralities based on the sequence of CDW intensity,[27,48,51] and to observe it experimentally. However, the presence of TRSB in the CDW of AV_3Sb_5 system remains contentious, as different experimental techniques have yielded conflicting results.[27,31,32,45,47–58]

Recently, a novel CDW order has also been discovered deep inside the antiferromagnetic (AFM) phase of kagome magnet FeGe,[59–67] which develops an A-type AFM order below 410 K with in-plane ferromagnetic coupling and interlayer AFM couplings and then undergoes a CDW phase transition at $\sim$ 110 K.[59–61] The CDW was suggested to be chiral based on neutron scattering and STM studies,[59,60] potentially related to the chiral flux phase as that in AV_3Sb_5 family. However, they mainly studied the short-range CDW in the as-grown FeGe crystals,[59,60,67] which have strong phase separation and a large amount of defects that may confuse the judgement of an intrinsic chiral CDW in FeGe. Until recently, we found that the sample quality of FeGe can be greatly improved by post-annealing treatment, and a long-range CDW can be obtained.[64–66,68] Here, we revisit the presence of the chiral CDW in post-annealed FeGe crystals by STM. Different from previous studies, our STM measurements reveal an isotropic long-range CDW without obvious symmetry breaking in the post-annealed FeGe. Meanwhile, we find that local RSB appears for the short-range CDW in the as-grown FeGe, which may be related to the structural disorders. Furthermore, the short-range CDW is inert to the applied external magnetic field and the detailed spin arrangements in FeGe, inconsistent with the expectation of a chiral CDW associated with chiral flux. Our results rule out the existence of spontaneous chiral and rotational symmetry breaking in the CDW state of FeGe, putting strong constraints on the further understanding of CDW mechanism in FeGe.

2. Methods

In our study, two FeGe crystals were studied, one is the as-grown FeGe with a short-range CDW (labeled as sample #S), the other one is the post-annealed FeGe at 320 °C, which exhibits a long-range CDW (labeled as sample #L). The influence of annealing treatments on CDW behavior has been described in detail in Refs. [64–66,68]. For STM measurements, FeGe crystals were mechanically cleaved at 80 K in ultrahigh vacuum with a base pressure better than 1×10^{-10} mbar and immediately transferred into a UNISOKU cryogenic STM at $T = 4.2$ K. Pt–Ir tips were used after being treated on a clean Au (111) substrate. Spin-polarized tips were prepared by manually indenting the tips into the FeGe surface.[59,69,70] The topographic images were acquired in constant-current mode. The $\mathrm{d}I/\mathrm{d}V$ spectra were collected by a standard lock-in technique with a modulation frequency of 973 Hz and a typical modulation amplitude ΔV of 20–30 mV at 4.2 K. The $\mathrm{d}I/\mathrm{d}V$ maps at different energies were collected by using the corresponding voltages as the setpoint conditions to minimize the setpoint effect.

3. Experimental results

3.1. Isotropic long-range CDW in sample #L

To reveal the intrinsic character of CDW in FeGe, we first examine sample #L with a long-range CDW, where the influence of phase inhomogeneity and structural disorders can be excluded as much as possible. Figure 1(a) displays the typical topographic image of a sample region in Fe_3Ge kagome layer (its determination has been discussed in our previous work[64,67]), containing two Fe_3Ge terraces separated by a single-unit-cell-height step of $\sim$ 4 Å (Fig. 1(b)). The long-range CDW is clearly demonstrated in the $\mathrm{d}I/\mathrm{d}V$ map of the same sample region (Fig. 1(c)). We then explore whether the previously observed symmetry breaking in AV_3Sb_5 family is present in the CDW state of FeGe. For RSB, we expect to see a preferred direction with much stronger or weaker CDW intensity than the other two propagation directions over a wide energy range. For TRSB induced by orbital magnetism, we anticipate a chiral distribution of the CDW intensities along three propagation directions over a wide energy range, with the chirality that is defined as the counting direction from the lowest to the highest (clockwise or anticlockwise) reversed under opposite magnetic field directions or in different domains/terraces with opposite spin orientations.[45,46,60]

To extract the CDW intensity, we obtain the fast Fourier transformation (FFT) images of the $\mathrm{d}I/\mathrm{d}V$ maps for separate Fe_3Ge terraces, as shown in Figs. 1(d) and 1(e). Three sets of strong and sharp 2×2 CDW spots are clearly resolved for both terraces, as enclosed by the colored circles and labeled as $Q^1_{2a_0}$ $Q^2_{2a_0}$ and $Q^3_{2a_0}$, respectively. Figures 1(f) and 1(g) show the intensity profiles along the three lattice directions, it is found that the full widths at half maximum (FWHM) of all the CDW peaks are comparable to those of Bragg peaks of the underlying lattice, further confirming the long-range nature of the CDW. For both sample regions, the CDW intensity, defined as the intensity of CDW spots in the FFT image and labeled as I, follows the tendency of $I_1 \approx I_2 \approx I_3$ at $E = 0.3$ eV, which suggests an isotropic CDW. To confirm this, we track the energy dependence of CDW intensity for both terraces, with the results shown in Figs. 1(h) and 1(i). For both terraces, the difference in CDW intensity for $Q^i_{2a_0}$ ($i = 1, 2, 3$) is most pronounced at $E = 0.2$ eV, but becomes very small at other energies. Moreover, the relative intensity for the three propagation directions varies with energy. These behaviors differ from the anisotropic or chiral CDW in AV_3Sb_5 family,[27,47,48] suggest-

ing an isotropic CDW without significant symmetry breaking in FeGe. A closer examination of the dI/dV maps in Fig. 1(c) reveals that the local distribution of CDW near defects (dark spots) exhibits a certain degree of anisotropy, which might contribute to the observed weak CDW anisotropy. Specific selectivity of STM tips might be another reason.

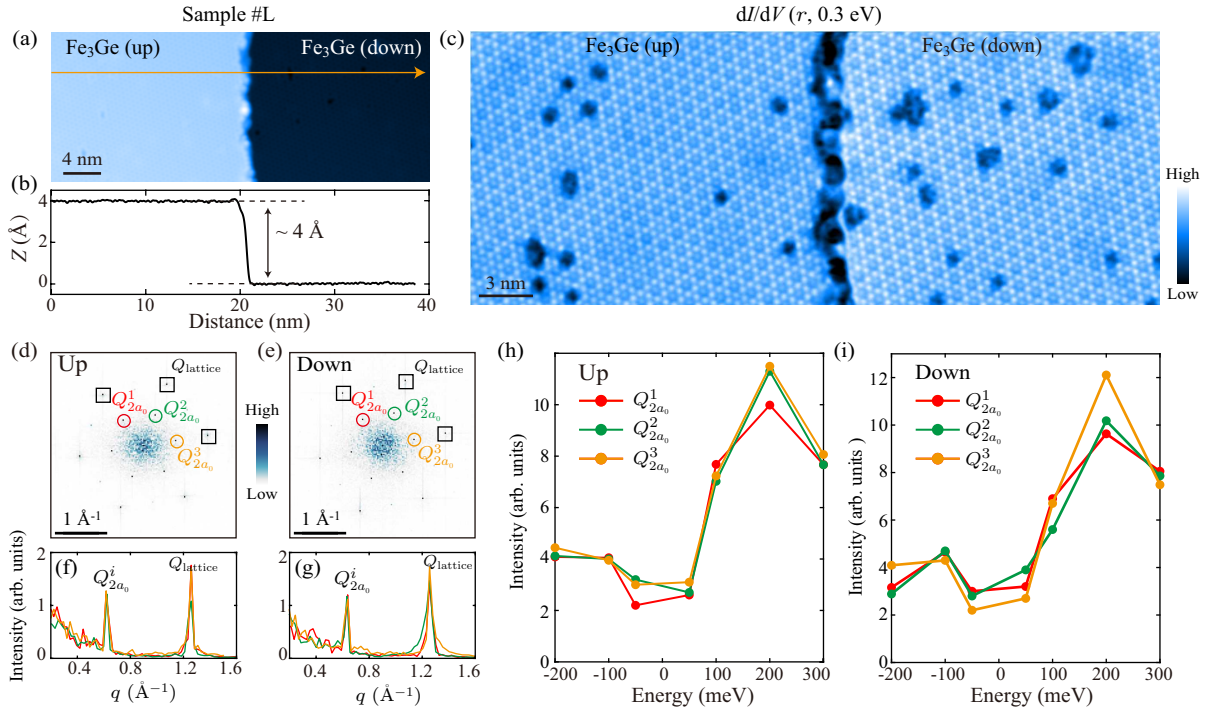


Fig. 1. Experimental evidence for an isotropic long-range CDW in sample #L. (a) Typical topographic image of Fe_3Ge layer, including a single-unit-cell-height step. (b) Height profile along the orange line in panel (a). (c) Typical dI/dV map of the same sample region shown in panel (a). (d), (e) FFT images of the dI/dV maps for up and down Fe_3Ge terraces in panel (c). The Bragg spots of CDW and underlying atomic lattice are enclosed by circles and rectangles, respectively. Three sets of CDW spots are labeled as $Q^1_{2a_0}$, $Q^2_{2a_0}$ and $Q^3_{2a_0}$, respectively. (f), (g) Line profiles of FFT intensity along the three lattice directions for up and down terraces, respectively. (h), (i) Energy dependence of CDW intensities for $Q^1_{2a_0}$, $Q^2_{2a_0}$ and $Q^3_{2a_0}$. Measurement conditions: (a) $V_b = 0.3$ V, $I_t = 300$ pA; (c) $V_b = 0.3$ V, $I_t = 300$ pA, $\Delta V = 20$ mV, $B = 0$ T.

3.2. Local rotational symmetry breaking of the short-range CDW in sample #S

Since our study suggests an isotropic long-range CDW in sample #L, a natural question arises: how to reconcile this with the previously reported chiral CDW in as-grown FeGe?[60] To address this, we conduct the same measurements on the as-grown FeGe (sample #S) using both Pt–Ir tips and spin-polarized FeGe tips. Unless specified, the following presented data were measured by spin-polarized tips; the related datasets measured by Pt–Ir tips are present in Section S1 of the supplementary materials (SM).

Figure 2(a) shows a typical dI/dV map of Fe_3Ge layer in sample #S, containing two Fe_3Ge terraces separated by a single-unit-cell-height step. Two distinct features are revealed. Firstly, the down Fe_3Ge terrace shows a much higher density of states (DOS) than the up Fe_3Ge terrace, confirming spin-polarized tunneling into different spin-polarized bands in adjacent kagome layers. This is consistent with the A-type AFM structure of FeGe, characterized by in-plane ferromagnetic coupling and interlayer AFM couplings.[59] More datasets and discussions for spin-polarized measurements are displayed in Section S2 of SM. Secondly, distinct from the post-annealed sample #L, sample #S exhibits strong phase separation between the 2×2 CDW and the initial undistorted 1×1 lattice, resulting in a short-range CDW. This is further demonstrated by the broadened CDW spots in FFT images (Figs. 2(b) and 2(c)) and the larger FWHM of CDW peaks in FFT line profiles (Figs. 2(d) and 2(e)), comparing to those of underlying atomic lattice.

We then check the existence of RSB and TRSB in sample #S. Figures 2(f) and 2(g) show the energy dependence of CDW intensities along three propagation directions for both Fe_3Ge terraces. For each Fe_3Ge terrace, the CDW intensities for all $Q^i_{2a_0}$ are closely aligned and exhibit a nearly identical trend in their relative difference between ± 0.4 eV, i.e., $I_1 > I_2 > I_3$. This seems to suggest the presence of rotational symmetry breaking or a chiral CDW in sample #S. However, if a chiral CDW does exist, the weak orbital magnetism induced by Berry curvature would couple to the internal magnetic field of in-plane ferromagnetism, exhibiting a staggered chirality between adjacent kagome layers. However, here in our study, the CDW chirality remains consistent for both up and down Fe_3Ge terraces over a wide energy range, contradicting previous STM studies that reported opposite chirality on adjacent Fe_3Ge terraces.[60] Moreover, the opposite chirality on adjacent Fe_3Ge terraces is also absent for a long-range CDW in

sample #L, as shown in Figs. 1(h) and 1(i).

The above discussions are based on spatially averaged results over a large sample region. However, the CDW is short-range in sample #S, thus we analyze the CDW behavior in a single domain. A closer look at Fig. 3(a) reveals that the CDW in some small domains exhibits distinct unidirectional behavior, and even stripe-like in certain regions; the preferred orientation changes in different domains, as indicated by the colored arrows. These observations can rule out the artificial effects induced by specific tip shapes, which generally result in a preferred orientation across the whole sample region. Therefore, our results reveal local RSB of the short-range CDW in sample #S. Furthermore, these findings have been confirmed by using a metal Pt–Ir tip (see Section S1 of SM for more details), ruling out the influence of spin selectivity.

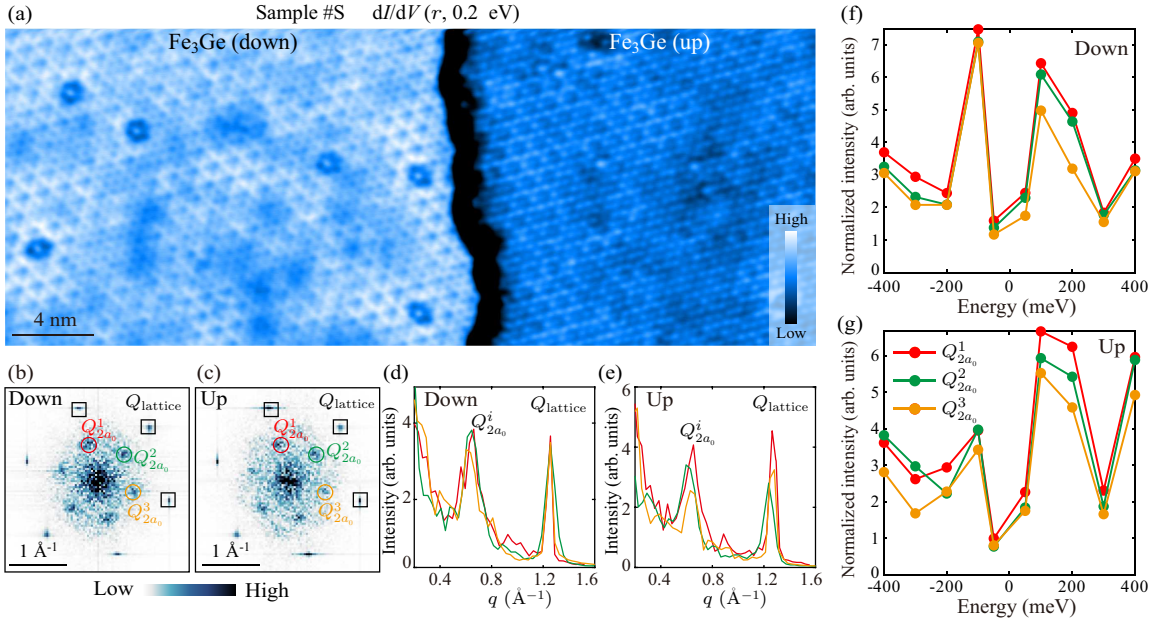


Fig. 2. Spatially averaged anisotropy of the short-range CDW in sample #S. (a) Typical dI/dV map of Fe_3Ge layer, including a single-unit-cell-height step. (b), (c) FFT images of the dI/dV maps for up and down Fe_3Ge terraces in panel (a). (d), (e) Line profiles of FFT intensity along the three lattice directions for up and down terraces. (f), (g) Energy dependence of CDW intensities for $Q^1_{2a_0}$, $Q^2_{2a_0}$ and $Q^3_{2a_0}$. Measurement conditions: (a) $V_b = 0.2$ V, $I_t = 300$ pA, $\Delta V = 30$ mV, $B = 0$ T.

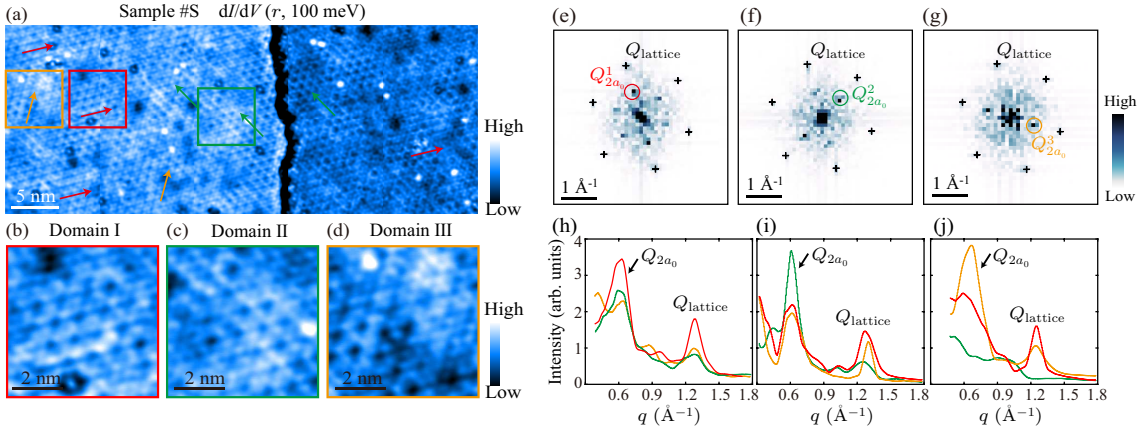


Fig. 3. Presence of local rotational symmetry breaking in the short-range CDW of sample #S. (a) Typical dI/dV map of Fe_3Ge layer, including a single-unit-cell-height step. Unidirectional CDWs along different orientations are observed in different domains, as indicated by the colored arrows. (b)–(d) Enlarged views of three CDW domains, as enclosed by the colored rectangles in panel (a). (e)–(g) Corresponding FFT images of panels (b)–(d), with the strongest CDW spots in each image enclosed by the colored circles. The Bragg spots of underlying atomic lattice are labeled by the black crosses. (h)–(j) Line profiles of FFT intensity along three lattice directions for panels (e)–(g), respectively. Measurement conditions: (a) $V_b = 0.1$ V, $I_t = 300$ pA, $\Delta V = 30$ mV, $B = 0$ T.

To be more quantitative, we select three CDW domains as examples. Their enlarged dI/dV maps are shown in Figs. 3(b)–3(d), with the corresponding FFT images displayed in Figs. 3(e)–3(g). In each domain, one of the CDW components is significantly stronger than the other two, as highlighted by the colored circles in Figs. 3(e)–3(g). Figures 3(h)–3(j) show the line profiles of FFT intensity along three lattice directions for the three domains, respectively. The relative intensity of three sets of $Q_{lattice}$ is the same for all three domains, but the relative intensity of three sets of CDW spots varies significantly. This confirms that the observed local RSB is genuine and not merely inherited from the properties of the under-

lying lattice. Additionally, these three domains are located on the same Fe_3Ge terrace, possessing the same spin orientation and similar DOS intensity (Fig. 3(a)), which indicates that the local RSB of CDW is independent of the spin orientation in Fe_3Ge layer.

We further investigate the response of CDW distribution to energy and magnetic field. Taking domain II as an example, Figs. 4(a) and 4(b) show two representative dI/dV maps at different energies, with the corresponding FFT images shown in Figs. 4(c) and 4(d). Obviously, the intensity of $Q^2_{2a_0}$ is higher than the other two CDW components at both energies. This behavior is also consistent over a wider energy range, as illustrated in Fig. 4(e), confirming the presence of RSB.

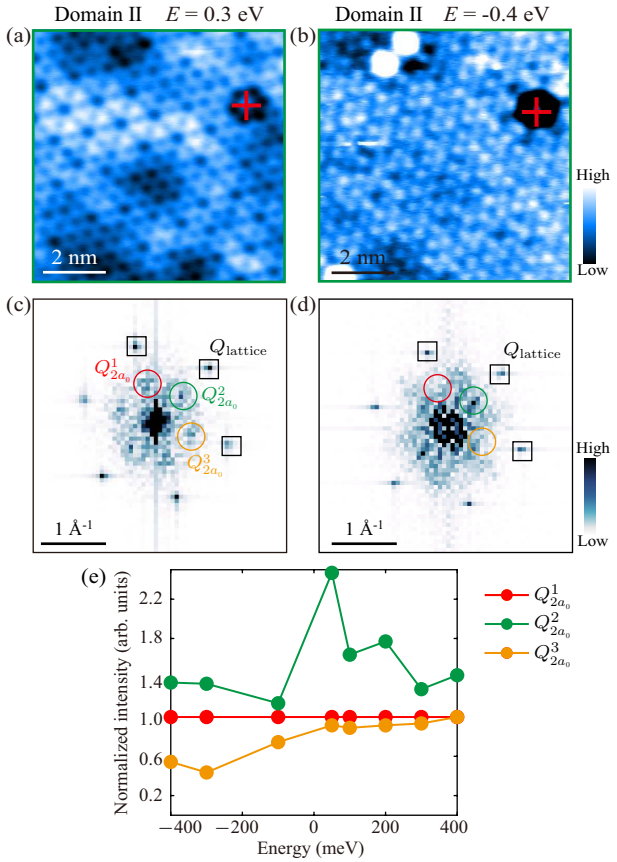


Fig. 4. Energy dependence of the CDW intensity in domain II of sample #S. (a), (b) Typical dI/dV maps of domain II at $E = 0.3$ eV and -0.4 eV, respectively. (c), (d) Corresponding FFT images of panels (a) and (b). (e) Energy dependence of normalized CDW intensities for $Q^1_{2a_0}$, $Q^2_{2a_0}$ and $Q^3_{2a_0}$. The intensity of CDW spots is normalized by that of $Q^1_{2a_0}$ for clarity. Measurement conditions: (a) $V_b = 0.3$ V, $I_t = 300$ pA, $\Delta V = 30$ mV, $B = 0$ T; (b) $V_b = -0.4$ V, $I_t = 300$ pA, $\Delta V = 30$ mV, $B = 0$ T.

According to the previous studies on AV_3Sb_5 and FeGe,[27,47,60] applying magnetic field might be an effective way to investigate the relationship between CDW and magnetism, as well as to distinguish TRSB from RSB, since the former is sensitive to magnetic field while the latter would not be. Here we applied magnetic fields ranging from -14 T to 14 T to check the evolution of the CDW intensity, with the maximum field of 14 T exceeding the threshold value needed for FeGe to spin flop.[59] Two representative dI/dV maps measured at $B = 1$ T and 14 T for the same sample region are displayed in Figs. 5(a) and 5(b). At $B = 1$ T, DOS contrast is obvious between the up and down Fe_3Ge terraces, but is almost absent at $B = 14$ T. This is because the tip spin is always along the c-axis, preventing the resolution of in-plane spin orientations (please see Section S2 of SM for more details). The unidirectional CDWs in different domains, as highlighted by the colored arrows in Figs. 5(a) and 5(b), have no response to the applied magnetic fields, although the spin configuration of FeGe has changed with magnetic fields. Figure 5(c) tracks the evolution of CDW intensities for different $Q^i_{2a_0}$ in domain II as a function of magnetic field at a fixed energy of $E = 0.1$ eV. The intensity of $Q^2_{2a_0}$ is always the strongest, and the so-called chirality of CDW remains unchanged for both positive and negative magnetic fields. Such inert responses of CDW in FeGe to magnetic structure and external magnetic field are more consistent with electronic nematicity (i.e., RSB) rather than TRSB.

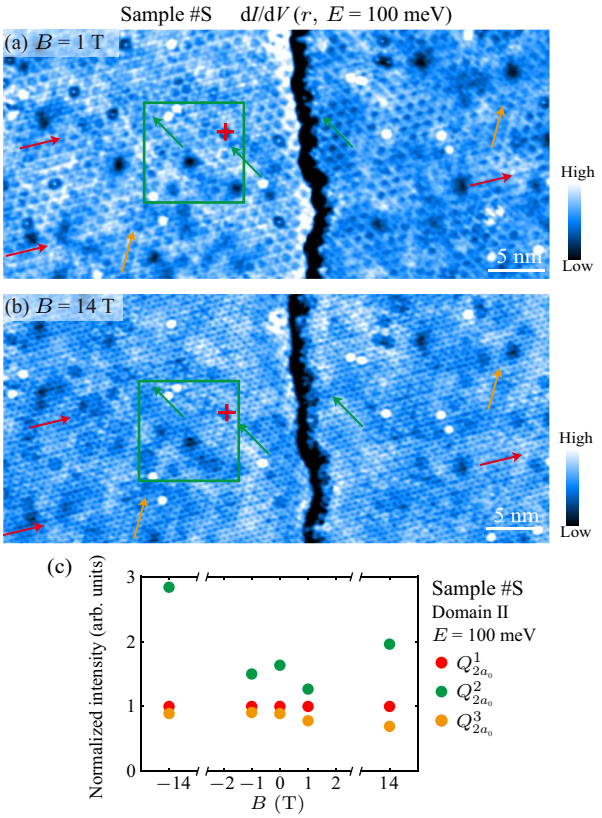


Fig. 5. Magnetic field dependence of CDW intensity in domain II of sample #S. (a), (b) Typical dI/dV maps measured at $B = 1$ T and 14 T for the same sample region. (c) Evolution of normalized CDW intensities for $Q^1_{2a_0}$, $Q^2_{2a_0}$ and $Q^3_{2a_0}$ as a function of B. The CDW intensities are normalized by that of $Q^1_{2a_0}$ for clarity. Measurement conditions: (a) $V_b = 0.1$ V, $I_t = 200$ pA, $\Delta V = 20$ mV, $B = 1$ T; (b) $V_b = 0.1$ V, $I_t = 200$ pA, $\Delta V = 20$ mV, $B = 14$ T.

4. Conclusion and perspectives

By systematical STM studies on the long- and short-range CDWs in FeGe, we do not find convincing evidence to support the presence of RSB or TRSB in the long-range CDW; however, local RSB is present for the short-range CDW. Neutron

scattering experiments have revealed that the CDW in FeGe is robust against spin canting at low temperatures and spin flop at high magnetic fields,[59] which is consistent with our STM results. Moreover, we find that the CDW distribution, particularly the preferred direction of RSB in the short-range CDW, is independent of both internal and external magnetic fields. These findings imply that the emergence of CDW in FeGe is not contingent upon the details of spin arrangements, which provides crucial clues to further understand the CDW mechanism in FeGe.

Our results differ from the observed CDW chirality regulated by the orientations of external magnetic fields in AV_3Sb_5 family and by the spin orientations in FeGe.[27,48,60] It is suggested that the CDWs in AV_3Sb_5 family and FeGe are topological, which are often accompanied with Berry curvature induced weak orbital magnetism.[40,68] The direction of orbital magnetism can be polarized by either an external magnetic field or the internal magnetic order, thus resulting in the chirality of CDW distribution. Currently, the existence of a chiral CDW in AV_3Sb_5 family is still under strong debates,[27,45,47,48,56,71] and our STM study does not support a chiral CDW in kagome magnet FeGe. Experimental signatures of chirality have been reported for the short-range CDW in the as-grown FeGe.[60] However, here we find that the long-range CDW is isotropic, and the short-range CDW in small domains breaks rotational symmetry, with the unidirectional behavior varying across domains on a single Fe_3Ge terrace. The selection of specific CDW domains on adjacent Fe_3Ge terraces may result in the coincidental chirality inversion. Our results suggest that there is no spontaneous time-reversal symmetry breaking or chiral symmetry breaking in the CDW state of FeGe, and put strong constraints on the presence of orbital magnetism in FeGe, which may not exist or may be even weaker than that in AV_3Sb_5 system if existed.

Finally, we try to understand the local RSB of the short-range CDW. Similar RSB has been observed in other CDW materials, such as 1T-$TiSe_2$ and 2H-$NbSe_2$. For 1T-Cu_xTiSe_2, the intercalated Cu atoms shorten significantly the in-plane correlation length of the CDW and even induce stripe CDW.[72] Such a stripe CDW can also be induced in 2H-$NbSe_2$ by local strain.[18] In our previous study, we found that the occurrence of CDW in FeGe is accompanied by a first-order structural transition with one quarter of Ge1 atoms in the kagome layers dimerized along the c-axis. Annealing treatments at different temperatures can tune the degree of Ge1-site disorder to obtain a long- or short-range CDW.[64] In the as-grown samples (sample #S here), the large amount of disorders in Ge1-sites prevent the formation of large domains with $1/4$ Ge1-dimerization, resulting in nanoscale phase separation and a short-range CDW.[64,67] We speculate that the strong phase separation and numerous defects in FeGe may induce strong disorder effect and local strain, responsible for the emergence of local RSB. The exact origin of local RSB for the short-range CDW in FeGe needs further theoretical and experimental investigations.

Acknowledgements

Project supported by the National Natural Science Foundation of China (Grant Nos. 12374140, 12494593, 11790312, 12004056, 11774060, and 92065201), the National Key R&D Program of China (Grant No. 2023YFA1406304), the Innovation Program for Quantum Science and Technology (Grant No. 2021ZD0302803), the Fundamental Research Funds for the Central Universities of China (Grant Nos. 2022CDJXY-002 and WK9990000103), and the New Cornerstone Science Foundation.

References

[1] Binder K and Young A P 1986 *Rev. Mod. Phys.* **58** 801
[2] Fiebig M 2005 *J. Phys. D: Appl. Phys.* **38** R123
[3] Phillips P 2012 *Advanced Solid State Physics* (Cambridge: Cambridge University Press) p. 34
[4] Novoselov K S, Mishchenko A, Carvalho A and Castro Neto A H 2016 *Science* **353** aac9439
[5] Bardeen J, Cooper L N and Schrieffer J R 1957 *Phys. Rev.* **108** 1175
[6] Fernandes R M, Chubukov A V and Schmalian J 2014 *Nat. Phys.* **10** 97
[7] Keimer B, Kivelson S A, Norman M R, Uchida S and Zaanen J 2015 *Nature* **518** 179
[8] Si Q, Yu R and Abrahams E 2016 *Nat. Rev. Mater.* **1** 16017
[9] Matsuyama K and Greensite J 2019 *Phys. Rev. B* **100** 184513
[10] Wise W D, Boyer M C, Chatterjee K, Kondo T, Takeuchi T, Ikuta H, Wang Y and Hudson E W 2008 *Nat. Phys.* **4** 696
[11] Comin R, Sutarto R, He F, Da Silva Neto E H, Chauviere L, Fraño A, Liang R, Hardy W N, Bonn D A, Yoshida Y, Eisaki H, Achkar A J, Hawthorn D G, Keimer B, Sawatzky G A and Damascelli A 2015 *Nat. Mater.* **14** 796
[12] Miao H, Fumagalli R, Rossi M, Lorenzana J, Seibold G, Yakhou-Harris F, Kummer K, Brookes N B, Gu G D, Braicovich L, Ghiringhelli G and Dean M P M 2019 *Phys. Rev. X* **9** 031042
[13] Wang N, Gu Y, McGuire M A, Yan J, Shi L, Cui Q, Chen K, Wang Y, Zhang H, Yang H, Dong X, Jiang K, Hu J, Wang B, Sun J and Cheng J 2022 *Chin. Phys. B* **31** 017106
[14] Chen Z, Li D, Lu Z, Liu Y, Zhang J, Li Y, Yin R, Li M, Zhang T, Dong X, Yan Y J and Feng D L 2023 *Nat. Commun.* **14** 2023
[15] Xue C L, Yuan Q Q, Xu Y J, Li Q Y, Dou L G, Jia Z Y and Li S C 2023 *Phys. Rev. B* **107** 134516
[16] Rice W D, Ambwani P, Bombeck M, Thompson J D, Haugstad G, Leighton C and Crooker S A 2014 *Nat. Mater.* **13** 481
[17] Santander-Syro A F, Fortuna F, Bareille C, Rödel T C, Landolt G, Plumb N C, Dil J H and Radović M 2014 *Nat. Mater.* **13** 1085
[18] Soumyanarayanan A, Yee M M, He Y, Van Wezel J, Rahn D J, Rossnagel K, Hudson E W, Norman M R and Hoffman J E 2013 *Proc. Natl. Acad. Sci. USA* **110** 1623
[19] Liu Y, Wei T, He G, Zhang Y, Wang Z and Wang J 2023 *Nature* **618** 934
[20] Ortiz B R, Gomes L C, Morey J R, Winiarski M, Bordelon M, Mangum J S, Oswald I W H, Rodriguez-Rivera J A, Neilson J R, Wilson S D, Ertekin E, McQueen T M and Toberer E S 2019 *Phys. Rev. Mater.* **3** 094407
[21] Ortiz B R, Teicher S M L, Hu Y, Zuo J L, Sarte P M, Schueller E C, Abeykoon A M M, Krogstad M J, Rosenkranz S, Osborn R, Seshadri R, Balents L, He J and Wilson S D 2020 *Phys. Rev. Lett.* **125** 247002
[22] Zhao H, Li H, Ortiz B R, Teicher S M L, Park T, Ye M, Wang Z, Balents L, Wilson S D and Zeljkovic I 2021 *Nature* **599** 216
[23] Chen H, Yang H, Hu B, Zhao Z, Yuan J, Xing Y, Qian G, Huang Z, Li G, Ye Y, Ma S, Ni S, Zhang H, Yin Q, Gong C, Tu Z, Lei H, Tan H, Zhou S, Shen C, Dong X, Yan B, Wang Z and Gao H J 2021 *Nature* **599** 222

[24] Ortiz B R, Sarte P M, Kenney E M, Graf M J, Teicher S M L, Seshadri R and Wilson S D 2021 *Phys. Rev. Mater.* **5** 034801
[25] Neupert T, Denner M M, Yin J X, Thomale R and Hasan M Z 2022 *Nat. Phys.* **18** 137
[26] Meng Y X, Xue C L, Dou L G, Zhao W M, Wang Q W, Xu Y J, Liu X, Xia W, Guo Y and Li S C 2023 *Chin. Phys. B* **32** 096801
[27] Jiang Y X, Yin J X, Denner M M, Shumiya N, Ortiz B R, Xu G, Guguchia Z, He J, Hossain M S, Liu X, Ruff J, Kautzsch L, Zhang S S, Chang G, Belopolski I, Zhang Q, Cochran T A, Multer D, Litskevich M, Cheng Z J, Yang X P, Wang Z, Thomale R, Neupert T, Wilson S D and Hasan M Z 2021 *Nat. Mater.* **20** 1353
[28] Liang Z, Hou X, Zhang F, Ma W, Wu P, Zhang Z, Yu F, Ying J J, Jiang K, Shan L, Wang Z and Chen X H 2021 *Phys. Rev. X* **11** 031026
[29] Luo H, Gao Q, Liu H, Gu Y, Wu D, Yi C, Jia J, Wu S, Luo X, Xu Y, Zhao L, Wang Q, Mao H, Liu G, Zhu Z, Shi Y, Jiang K, Hu J, Xu Z and Zhou X J 2022 *Nat. Commun.* **13** 273
[30] Xiang Y, Li Q, Li Y, Xie W, Yang H, Wang Z, Yao Y and Wen H H 2021 *Nat. Commun.* **12** 6727
[31] Mielke C, Das D, Yin J X, Liu H, Gupta R, Jiang Y X, Medarde M, Wu X, Lei H C, Chang J, Dai P, Si Q, Miao H, Thomale R, Neupert T, Shi Y, Khasanov R, Hasan M Z, Luetkens H and Guguchia Z 2022 *Nature* **602** 245
[32] Yu L, Wang C, Zhang Y, Sander M, Ni S, Lu Z, Ma S, Wang Z, Zhao Z, Chen H, Jiang K, Zhang Y, Yang H, Zhou F, Dong X, Johnson S L, Graf M J, Hu J, Gao H J and Zhao Z 2021 arXiv:2107.10714
[33] Nie L, Sun K, Ma W, Song D, Zheng L, Liang Z, Wu P, Yu F, Li J, Shan M, Zhao D, Li S, Kang B, Wu Z, Zhou Y, Liu K, Xiang Z, Ying J, Wang Z, Wu T and Chen X 2022 *Nature* **604** 59
[34] Ratcliff N, Hallett L, Ortiz B R, Wilson S D and Harter J W 2021 *Phys. Rev. Mater.* **5** L111801
[35] Tan H, Liu Y, Wang Z and Yan B 2021 *Phys. Rev. Lett.* **127** 046401
[36] Hu Y, Wu X, Ortiz B R, Han X, Plumb N C, Wilson S D, Schnyder A P and Shi M 2022 *Phys. Rev. B* **106** L241106
[37] Broyles C, Graf D, Yang H, Dong X, Gao H and Ran S 2022 *Phys. Rev. Lett.* **129** 157001
[38] Frassineti J, Bonfà P, Allodi G, Garcia E, Cong R, Ortiz B R, Wilson S D, De Renzi R, Mitrović V F and Sanna S 2023 *Phys. Rev. Res.* **5** L012017
[39] Kang M, Fang S, Yoo J, Ortiz B R, Oey Y M, Choi J, Ryu S H, Kim J, Jozwiak C, Bostwick A, Rotenberg E, Kaxiras E, Checkelsky J G, Wilson S D, Park J H and Comin R 2022 *Nat. Mater.* **22** 186
[40] Wang Y, Wu T, Li Z, Jiang K and Hu J 2023 *Phys. Rev. B* **107** 184106
[41] Wu P, Tu Y, Wang Z, Yu S, Li H, Ma W, Liang Z, Zhang Y, Zhang X, Li Z, Yang Y, Qiao Z, Ying J, Wu T, Shan L, Xiang Z, Wang Z and Chen X 2023 *Nat. Phys.* **19** 1143
[42] Feng X, Jiang K, Wang Z and Hu J 2021 *Science Bulletin* **66** 1384
[43] Denner M M, Thomale R and Neupert T 2021 *Phys. Rev. Lett.* **127** 217601
[44] Ma H Y, Yin J X, Zahid Hasan M and Liu J 2024 *Chin. Phys. Lett.* **41** 047103
[45] Li H, Zhao H, Ortiz B R, Park T, Ye M, Balents L, Wang Z, Wilson S D and Zeljkovic I 2022 *Nat. Phys.* **18** 265
[46] Ishioka J, Liu Y H, Shimatake K, Kurosawa T, Ichimura K, Toda Y, Oda M and Tanda S 2010 *Phys. Rev. Lett.* **105** 176401
[47] Shumiya N, Hossain Md S, Yin J X, Jiang Y X, Ortiz B R, Liu H, Shi Y, Yin Q, Lei H, Zhang S S, Chang G, Zhang Q, Cochran T A, Multer D, Litskevich M, Cheng Z J, Yang X P, Guguchia Z, Wilson S D and Hasan M Z 2021 *Phys. Rev. B* **104** 035131
[48] Wang Z, Jiang Y X, Yin J X, Li Y, Wang G Y, Huang H L, Shao S, Liu J, Zhu P, Shumiya N, Hossain M S, Liu H, Shi Y, Duan J, Li X, Chang G, Dai P, Ye Z, Xu G, Wang Y, Zheng H, Jia J, Hasan M Z and Yao Y 2021 *Phys. Rev. B* **104** 075148
[49] Guo C, Wagner G, Putzke C, Chen D, Wang K, Zhang L, Gutierrez-Amigo M, Errea I, Vergniory M G, Felser C, Fischer M H, Neupert T and Moll P J W 2024 *Nat. Phys.* **20** 579
[50] Xing Y, Bae S, Ritz E, Yang F, Birol T, Capa Salinas A N, Ortiz B R, Wilson S D, Wang Z, Fernandes R M and Madhavan V 2024 *Nature* **631** 60
[51] Yu F H, Wu T, Wang Z Y, Lei B, Zhuo W Z, Ying J J and Chen X H 2021 *Phys. Rev. B* **104** L041103
[52] Kenney E M, Ortiz B R, Wang C, Wilson S D and Graf M J 2021 *J. Phys.: Condens. Matter* **33** 235801
[53] Khasanov R, Das D, Gupta R, Mielke C, Elender M, Yin Q, Tu Z, Gong C, Lei H, Ritz E T, Fernandes R M, Birol T, Guguchia Z and Luetkens H 2022 *Phys. Rev. Res.* **4** 023244
[54] Xu Y, Ni Z, Liu Y, Ortiz B R, Deng Q, Wilson S D, Yan B, Balents L and Wu L 2022 *Nat. Phys.* **18** 1470
[55] Wu Q, Wang Z X, Liu Q M, Li R S, Xu S X, Yin Q W, Gong C S, Tu Z J, Lei H C, Dong T and Wang N L 2022 *Phys. Rev. B* **106** 205109
[56] Li H, Wan S, Li H, Li Q, Gu Q, Yang H, Li Y, Wang Z, Yao Y and Wen H H 2022 *Phys. Rev. B* **105** 045102
[57] Saykin D R, Farhang C, Kountz E D, Chen D, Ortiz B R, Shekhar C, Felser C, Wilson S D, Thomale R, Xia J and Kapitulnik A 2023 *Phys. Rev. Lett.* **131** 016901
[58] Hu Y, Yamane S, Mattoni G, Yada K, Obata K, Li Y, Yao Y, Wang Z, Wang J, Farhang C, Xia J, Maeno Y and Yonezawa S 2023 arXiv:2208.08036
[59] Teng X, Chen L, Ye F, Rosenberg E, Liu Z, Yin J X, Jiang Y X, Oh J S, Hasan M Z, Neubauer K J, Gao B, Xie Y, Hashimoto M, Lu D, Jozwiak C, Bostwick A, Rotenberg E, Birgeneau R J, Chu J H, Yi M and Dai P A 2022 *Nature* **609** 490
[60] Yin J X, Jiang Y X, Teng X, Hossain Md S, Mardanya S, Chang T R, Ye Z, Xu G, Denner M M, Neupert T, Lienhard B, Deng H B, Setty C, Si Q, Chang G, Guguchia Z, Gao B, Shumiya N, Zhang Q, Cochran T A, Multer D, Yi M, Dai P and Hasan M Z 2022 *Phys. Rev. Lett.* **129** 166401
[61] Teng X, Oh J S, Tan H, Chen L, Huang J, Gao B, Yin J X, Chu J H, Hashimoto M, Lu D, Jozwiak C, Bostwick A, Rotenberg E, Granroth G E, Yan B, Birgeneau R J, Dai P and Yi M 2023 *Nat. Phys.* **19** 814
[62] Miao H, Zhang T T, Li H X, Fabbris G, Said A H, Tartaglia R, Yilmaz T, Vescovo E, Yin J X, Murakami S, Feng X L, Jiang K, Wu X L, Wang A F, Okamoto S, Wang Y L and Lee H N 2023 *Nat. Commun.* **14** 6183
[63] Shao S, Yin J X, Belopolski I, You J Y, Hou T, Chen H, Jiang Y, Hossain M S, Yahyavi M, Hsu C H, Feng Y P, Bansil A, Hasan M Z and Chang G 2023 *ACS Nano* **17** 10164
[64] Chen Z, Wu X, Zhou S, Zhang J, Yin R, Li Y, Li M, Gong J, He M, Chai Y, Zhou X, Wang Y, Wang A, Yan Y J and Feng D L 2024 *Nat. Commun.* **15** 6262
[65] Shi C, Liu Y, Maity B B, Wang Q, Kotla S R, Ramakrishnan S, Eisele C, Agarwal H, Noohinejad L, Tao Q, Kang B, Lou Z, Yang X, Qi Y, Lin X, Xu Z A, Thamizhavel A, Cao G H, Smaalen S van, Cao S and Bao J K 2024 *Sci. China Phys. Mech. Astron.* **67** 117012
[66] Wu X, Mi X, Zhang L, Wang C W, Maraytta N, Zhou X, He M, Merz M, Chai Y and Wang A 2024 *Phys. Rev. Lett.* **132** 256501
[67] Chen Z, Wu X, Yin R, Zhang J, Wang S, Li Y, Li M, Wang A, Wang Y, Yan Y J and Feng D L 2024 *Phys. Rev. B* **110** 245104
[68] Oh J S, Biswas A, Klemm M, Tan H, Hashimoto M, Lu D, Yan B, Dai P, Birgeneau R J and Yi M 2024 arXiv:2404.02231
[69] Bode M 2003 *Rep. Prog. Phys.* **66** 523
[70] Wiesendanger R 2009 *Rev. Mod. Phys.* **81** 1495
[71] Yin J X, Lian B and Hasan M Z 2022 *Nature* **612** 647
[72] Novello A M, Spera M, Scarfato A, Ubaldini A, Giannini E, Bowler D R and Renner Ch 2017 *Phys. Rev. Lett.* **118** 017002